NUMERICAL SIMULATION OF WORKING PROCESS IN RAMJET–TYPE PDE

V.V.Vlasenko
TsAGI
Zhukovsky, Russia
vvvlas@progtech.ru

A.A.Shiryaeva
TsAGI
Zhukovsky, Russia
anette_dc@mail.ru

Abstract. One concept of supersonic ramjet–scheme pulsing engine that had been studied numerically in [1]. Results of new parametric numerical investigations, intended to improve the characteristics of such PDE, are described. A new boundary condition on a perforated wall is used; this condition allows to describe in more details the process of gas flow through the perforation and to estimate the additional force that acts on the wall. Modifications of the PDE geometry are proposed in order to attain the value of useful force, which would be several times higher than outer drag, and to prevent the compression wave from coming into inlet. The results of the working cycle numerical simulation are presented for PDE with modified geometry. Estimations of possible thrust–efficiency characteristics and of the cyclical working process frequency are given. It is analyzed how various elements of the engine construction contribute to longitudinal force that acts on the PDE.

Keywords. Numerical simulation, Ramjet–scheme PDE, Aircraft engine, Parametrical calculations.

1 Introduction

The use of controlled process of pulsing detonation for effective fuel burning is considered to be one of the possible approaches in the development of aircraft engines. This problem is being widely studied in different scientific-research organizations and universities in the USA, Japan, Canada, France, Sweden, Russia and other countries. The stage of concrete project realization has begun – including demonstration and flight models. However, many questions of Pulsing Detonation Engine (PDE) operation are still studied insufficiently. One such question is the estimation PDE efficiency in comparison with traditional engines. Review of papers [2-4] demonstrates great variety of methods used for assessments, and quantitative results may differ by order.

PDE offers a number of advantages as compared to an ordinary engine (with a stationary operation process): there are no limitations of the energy, released during combustion process; unlike a usual ramjet, PDE may theoretically operate at any speed – starting from $M \approx 0$; it has a more effective thermodynamic cycle than a ramjet and a simpler construction than a turbo-jet engine has. The principal disadvantage of PDE is that passage of compression waves through the duct results in non-uniform (periodical) construction loadings with a very large amplitude. It may cause both the problems of the construction durability and the noise problems.

In the Central Aerohydrodynamic Institute named after N.E.Zhukovsky (TsAGI), the first concept of multi-chamber PDE was proposed by prof. I.S.Simonov (1991). Its characteristic feature is that

there are several detonation chambers which have common inlet and nozzle (i.e. “chambers in a chamber”) (see Figure1). Each detonation chamber includes an entrance region intended for subsonic inflow and a system of fuel injectors. Ignition of the gas mixture is performed in the region of outlet cross-section. To damp the shock wave inside the chambers, a perforated section is used; it is placed upstream from injectors. Cold air, passing between the chambers, cools them, and then is ejected and mixed with flowing out combustion products. In order to ensure the uniformity of combustion products at the nozzle entrance and to increase the frequency of engine operation, working cycles of individual chambers are time-shifted.

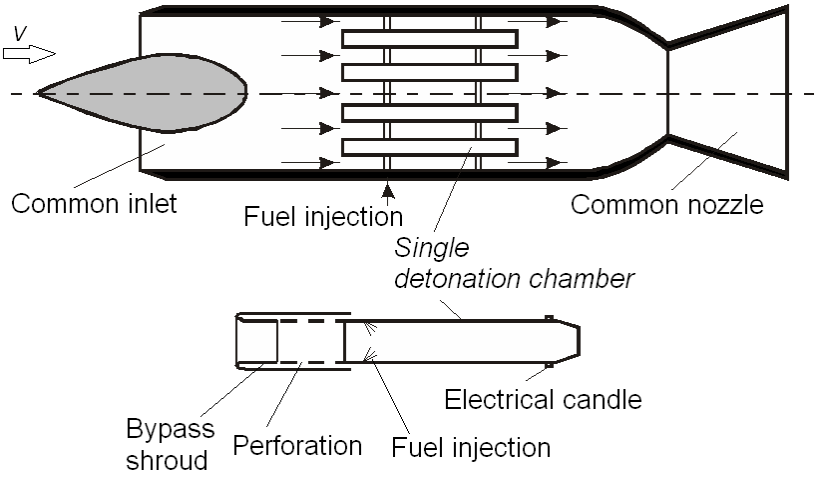

Figure 1: Concept “chambers in a chamber” by Prof. I.S.Simonov (1991).

To develop and improve the working process (and in particular – the interaction of inlet with combustor), an experimental setup DT-100 was created in TsAGI. During research work held with the use of setup DT-100, the means of reliable detonation initiation in a ramjet-scheme chamber were developed, and the shock damping in the combustor perforated section was explored.

In 2003 Dr. N.Kh.Remeev (TsAGI) proposed the concept of single-chamber supersonic ramjet-scheme PDE [5], designed for the main flight regime with Mach number $M = 3$. The scheme of this PDE concept is shown in Fig.2. The fuel (H_2) is injected directly to the airflow entering into a combustor. Detonation initiation is performed at the end of the chamber, upstream from the exhaust nozzle entry. At the same moment, fuel injection is stopped to avoid the beginning of diffusion combustion. After ignition, a detonation wave arises, which propagates upstream along the duct and burns the gas mixture in the combustor. Having reached the injection section, the detonation wave decays with formation of strong shock wave that propagates further upstream. The engine doesn’t use any devices for screening the combustor from the inlet. Hence an essential part of working cycle is the stage of the shock wave damping. This is necessary in order to avoid the destruction of the flow in the inlet by the shock wave. Besides, it’s possible to use the shock wave momentum in order to increase the axial force. To prevent this wave from the exit into the inlet, the bypass system is used. The gas compressed in the shock wave is bypassed through the perforated wall into the shroud, where it turns and outflows in the longitudinal direction. After the compression wave is suppressed and the flow in the PDE duct is restored, the hydrogen injection begins again and the cycle is repeated.

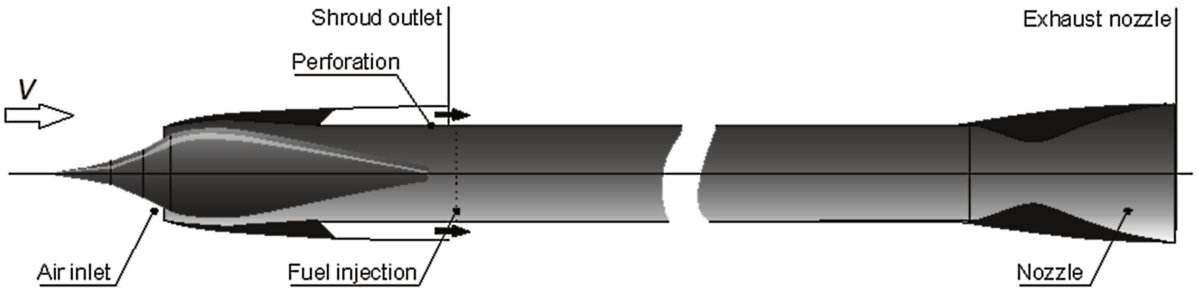

Figure 2: Concept of ramjet–scheme PDE by N.Kh.Remeev (2003).

In the current work, the results of research of the ramjet-scheme PDE working process possible characteristics are presented. The study was performed by means of numerical simulation.

2 Organization of calculations

Numerical simulation of working process in detonation engine was performed in approximation of axisymmetric flow on the basis of full non-stationary Reynolds equation system closed by $(q-\omega)$-model of turbulence and by Moretti kinetic scheme (which includes 8 reactions between 7 species) for the description of non-equilibrium hydrogen-air combustion. Viscous effects in the vicinity of chamber walls were excluded from consideration.

Numerical method, which has 2nd approximation order in all variables, was used. It includes explicit monotone Godunov-Kolgan_Rodionov scheme for approximation of convective fluxes, explicit modified central-difference scheme for approximation of diffusive fluxes and point-implicit approximation of source terms.

The modeling of the gas flowing through the perforated wall represents the most severe difficulty. The gas flow inside the bypass shroud and the flow in the main PDE duct were calculated simultaneously; special boundary condition was imposed on the perforated wall that separates these two flows. In the work [1] the "DT100" boundary condition was used. In that boundary condition, the perforated wall is considered as a linear superposition of a boundary with free interaction of flows and of a solid wall – with coefficients β and $(1-\beta)$, where β is the perforation ratio (relative area of perforation holes). The perforation holes were opened, when the pressure difference exceeded 10 atm. In the new calculations the perforation holes were always opened and boundary condition "PERFO" [6] was applied. The last version of boundary condition "PERFO" (2009) takes into account the form of perforated holes and the angle of their slope θ with respect to the positive direction of longitudinal axis (see fig.3). The holes are taken to be rectangles with dimensions $a \times b$. Besides, this boundary condition makes it possible to estimate additional longitudinal force that acts on perforated wall during the bypass of gas. Each perforation hole is regarded as a separate computational subregion consisting of one cell. The flow in the hole is considered as flat and inviscid. The parameters on the upper and lower borders of this cell are taken from the near-wall cells of computational subregions 1 and 2 (these subregions correspond to the main duct of PDE and to the bypass shroud). Because of non-stationary processes the parameters with indexes 1 and 2 change from one time step to another. Left and right borders are considered as solid walls. Parameters in a hole are determined from the solution of Euler equation system with Godunov scheme. At the same time, specific fluxes through the upper and lower borders of the hole are determined - $\vec{F}_{hole1}$ and $\vec{F}_{hole2}$. These fluxes are used in definition of numerical boundary condition in adjacent subregions of computational domain. The flux through the border of a mesh adjacent to the wall is computed as $\left[(1-\beta)\vec{F}_W + \beta\vec{F}_{hole}\right]\cdot 2\pi Rh$ ($\vec{F}_W$ - fluxes through the solid wall, R - the radius of the duct, h - the length of the mesh).

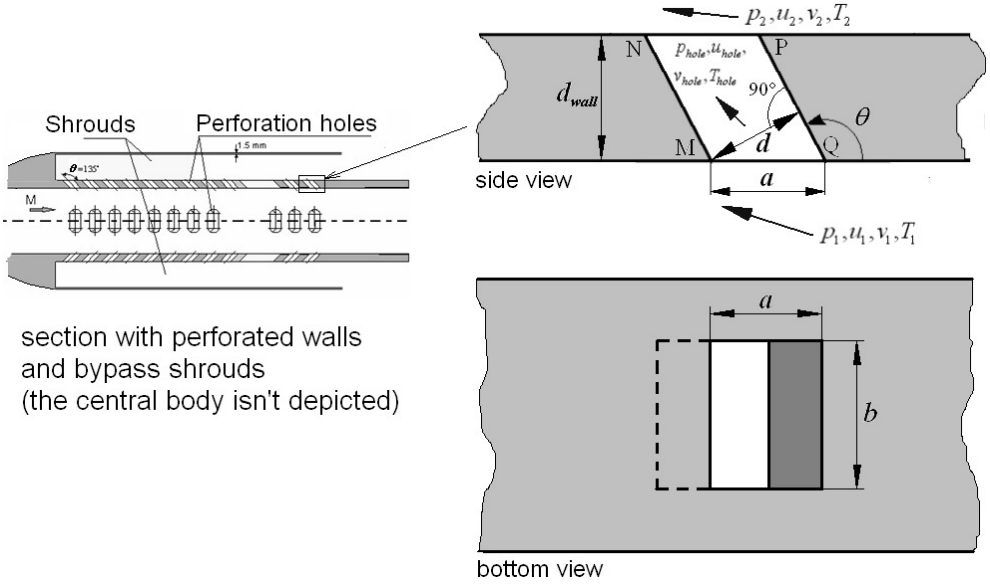

Figure 3: Simulation of gas flow through the perforation. Boundary condition “PERFO”.

3 Results of calculations

The work [1] describes the numerical simulation of working process for the PDE that is shown in Fig.2. Hydrogen was injected from walls, perpendicularly to the flow, through the circular slot in the combustor wall. Total pressure of hydrogen was equal to 10 atm. Width of the slot was chosen to get the given value of the air excess ratio α after the fuel mixing with air. The combustion ignition was performed by brief addition of energy to one cell of grid near the PDE duct axis (simulation of an electrical candle).

In those calculations, the cyclical working regime of the device had been obtained. It had been shown that the useful longitudinal force is produced by interaction of the compression wave with the central body and by the reflection of this wave from the end–wall of the bypass shroud. PDE characteristics, which had been obtained in calculations for the flight Mach number $M = 3$, the height $H = 20$ км and the air excess ratio $\alpha = 2$, are given in the first line of the Table 1. In this Table, t_{cycle} is the duration of one working cycle of the PDE; G_{fuel} is fuel consumption; R is useful integral longitudinal force, applied to all inner surfaces of PDE (including bypass shrouds), with the deduction of the ambient pressure; X is total integral longitudinal force, applied to all surfaces of PDE (both inner and outer); $J_{sp} = \langle R \rangle / \left(g \cdot \langle G_{fuel} \rangle \right)$ is specific impulse (g is acceleration of gravity); $C_R = \langle R \rangle / \left(q_\infty \cdot F_{\text{mid}} \right)$ and $C_X = \langle X \rangle / \left(q_\infty \cdot F_{\text{mid}} \right)$ are coefficients of forces R and X, accordingly ($q_\infty = \rho_\infty u_\infty^2 / 2$ is the dynamic pressure of ambient flow, F_{mid} is midship section area of PDE). Though the satisfactory values of the specific impulse and of the useful force coefficient had been obtained, the outer drag of the PDE had appeared to be higher than the useful force ($X < 0$). Moreover, the bypass device had been found to be unable to stop the running upstream compression wave, and for a short time this wave came out from the inlet.

In 2009–2010, new calculations of the ramjet–type PDE have been performed for the same flight regime. The advanced numerical technology was used. In addition, some modifications were

introduced sequentially to the PDE concept with the aim to increase the useful force and to prevent the compression wave from coming out of the inlet. Below the results of these calculations are demonstrated. Working process characteristics, obtained in these computations, are given in Table 1.

First series of calculations was performed for the same geometry of PDE as in the work [1] – variant 1 in Fig.4. As well as in [1], the perforation ratio was taken to be equal to $\beta = 0.2$. Results for angle of the perforation holes $\theta = 135°$ are given in the second line of the Table 1. One may see that the useful force $\langle R \rangle$ (averaged over a cycle) has even diminished, because the permanently-opened perforation produces drag during the prolonged stage of the PDE duct refilling by air after damping of the compression wave.

Variant	t_{cycle}, sec	$\langle G_{fuel} \rangle$, kg/sec	$\langle R \rangle$, N	$\langle X \rangle$, N	J_{sp}, sec	C_R	C_X
Variant "1", α=2, old boundary condition	0.0075220	0.001018	45.43	-3.56	4550	0.35	-0.03
Variant "1", α=1.8, β=0.2, θ=135°	0.0075220	0.001066	33.87	-1.98	3239	0.25	-0.02
Variant "1", α=1, β=0.2, θ=135°	0.0075220	0.001813	54.74	11.78	3078	0.40	0.09
Variant "1", α=1, β=0.2, θ=135°, shortened cycle	0.0067119	0.001594	65.57	19.55	4193	0.48	0.14
Variant "2", α =1, β =0.5, θ =90°	0.0094728	0.001123	212.51	170.48	19290	0.94	0.76
Variant "2", α =1, β =0.5, θ =135°	0.0092681	0.001190	232.89	178.36	19950	1.03	0.79
Variant"3" , α =0.8, β =0.5, θ =135°	0.0085000	0.001372	172.21	115.81	12794	0.76	0.51

Table 1: Integral characteristics, obtained for various variants of PDE.

In the engine configuration under consideration the perforated section is too short. As a result, the shock wave damping is insufficient. For the same reason, the angle and form of perforation holes and the force, acting on the perforated wall, have small influence. Noticeable variation of the PDE characteristics within the variant 1 has been obtained only through the increase of fuel consumption from $\alpha = 2$ (as in the work [1]) to $\alpha = 1$. As a result, the useful force has increased 1.6 times, and the total force $\langle X \rangle$ has become positive. However, the outer drag still remained to be comparable with the useful force $\langle R \rangle$, and the total longitudinal force $\langle X \rangle$ was nearly 5 times lower than the useful force $\langle R \rangle$. In addition, the bypass device still did not provide damping of the compression wave, and this wave came out of the inlet entrance – see the wave trajectories in Fig.5.

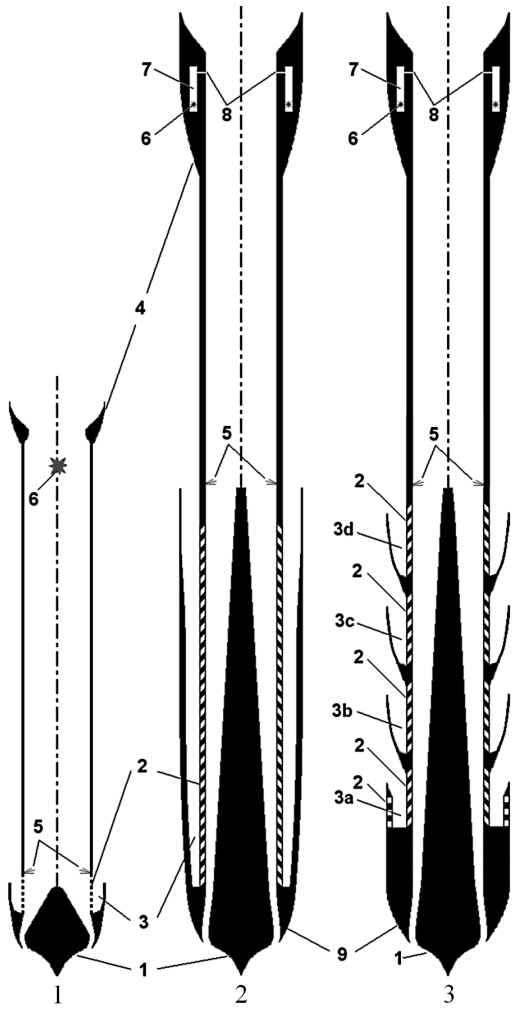

Figure 4: Variants of PDE geometry: 1 – central body; 2 – perforated wall; 3 – bypass shrouds (3a, 3b, 3c, 3d – various rings of shrouds); 4 – nozzle; 5 – hydrogen injection; 6 – ignition; 7 – circular initiator; 8 – slot of the initiator; 9 – cowl of the inlet. Scale in radial direction is expanded.

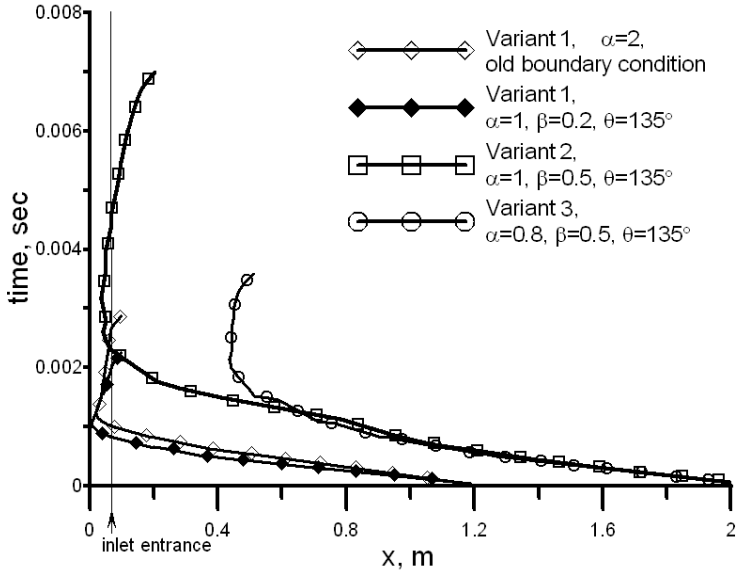

Figure 5: Trajectories of main compression wave for the most characteristic variants

Let us analyze different components of engine thrust. Figure 6 depicts the forces, which are applied to various surfaces of the engine and are contained in expression for the longitudinal force $\langle X \rangle$. From this plot it may be concluded that the nozzle itself doesn't produce force in positive direction. Thrust is created due to forces applied to the surface of central body (diffuser) and to inner walls of the bypass shroud. Front part of the central body (cone) diminishes the thrust; this effect is amplified, when the shock wave goes out from the inlet duct. Therefore, in the investigated variant of engine the thrust is mainly produced at the stage, when detonation or shock wave is inside the entrance part of the engine (during time interval $0.5\ \mu sec < t < 4\ \mu sec$). During the wave motion along the combustor ($t < 0.5\ \mu sec$) and during the combustor filling by fuel ($t > 4\ \mu sec$) the thrust is negative. It's obvious that average thrust could be increased, if the time of the chamber filling by fuel would be diminished and if the wave would be prevented from going out from the inlet duct.

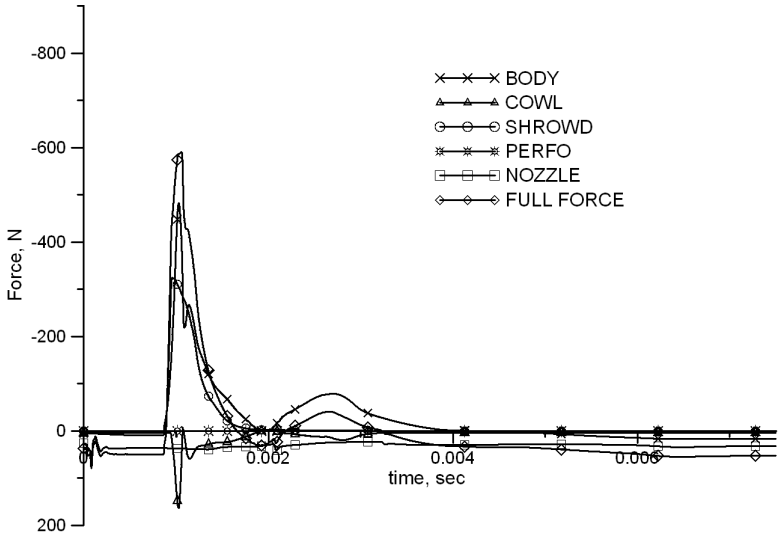

Figure 6: Balance of longitudinal forces for variant 1, α=1, β=0.2, θ=135º.

The principal stages of development of processes in a PDE duct obtained for the air excess ratio $\alpha = 2$ are depicted in Fig.7. In the beginning the maximal possible part of combustor volume was filled by fuel with the air excess ratio $\alpha = 2$ (Fig.7a, field of coefficient α). In the other parts of Fig.7 the temperature fields are shown for the following stages of the working cycle. Stages of ignition, detonation wave formation and its upstream propagation are represented by Fig.7b,c,d. Then the shock wave, produced by detonation, propagates to the inlet throat (Fig.7e), moves to the cowl leading edge (Fig.7f) and finally goes out (Fig.7g). Stages of shock wave return to the inlet duct and approaching of the closing shock to its initial position (where it was before the ignition) are shown in Fig.7h,i,j,k,l.

Let's consider in details the wave motion along the perforated section and the inlet. During the wave motion upstream, gas velocity after the wave front is directed to the left. When the wave goes out from the diffuser duct, intensive bypass of the gas begins, and the wave intensity diminishes quickly. At some moment, the wave appears to be so damped that the gas velocity after its front becomes positive. After that the slow backward motion of the wave begins. Damping of the wave is accompanied by the growth of gas velocity after its front. Finally, gas velocity in the inlet throat reaches the speed of sound, and region of supersonic flow arises in diffuser. Interaction of supersonic flow with still slowly moving gas in the perforated part produces new closing shock wave. The wave, which was initially produced by ignition, becomes more and more weak. When the new closing shock wave approaches to initial position of the previous closing shock (before the ignition), the hydrogen injection begins again. After that, closing shock wave continues to move downstream. When the air excess ratio in the nozzle region becomes equal to $\alpha = 1$, the new ignition is made.

Figure 7: PDE working cycle (fields of temperature in sequential time moments).

An important question is when the new cycle should be started (i.e. when the stopping of fuel injection and the new ignition should be performed). As it may be seen from the plot of longitudinal force, at the end of cycle the total force is negative; accordingly, it makes negative contribution to the averaged-over-cycle longitudinal force. In calculation of variant 1 with α=1 the fuel injection was stopped at the time moment $t = 0.007522$ sec. But the analysis of sequential flowfields has shown that the satisfactory filling of the chamber by fuel mixture was attained earlier – at the time moment $t = 0.006712$ sec. If one chooses this moment as the time of the first cycle finishing and of the new ignition, then the portion of the stage with negative longitudinal force would diminish, and the averaged-over-cycle longitudinal force would increase– see Table 1. Effect of shortening the "negative" stage appears to be even higher, because the averaged-over-cycle thrust is inversely proportional to the cycle duration, and shortening of this stage diminishes the cycle duration.

To improve the PDE characteristics, new variant of its geometry has been considered - variant 2 in Fig.4. Perforation ratio has been increased to $\beta = 0.5$, and length of the perforated section has been increased nearly 10 times. In addition, the convergent part of the nozzle has been removed (it produced additional drag). For relyable detonation generation, a circular initiator of detonation was also used instead of the electrical candle. It was placed inside the nozzle and was filled by

hydrogen-air mixture ($\alpha = 1.5$) under the pressure 12.89 atm. The mixture inside the initiator was ignited in the described above way, and the high–pressure combustion products came to the PDE main duct through a circular slot, which was opened, if the pressure difference across the wall was higher than 15 atm.

In Fig.8, the balance of longitudinal forces for variant 2 is plotted. Essential difference from previous geometry is evident: the nozzle produces thrust during almost the whole period of cycle; total integral longitudinal force is also positive almost throughout. As a result, the average useful force increased approximately 4 times and became approximately 4 times higher than outer drag.

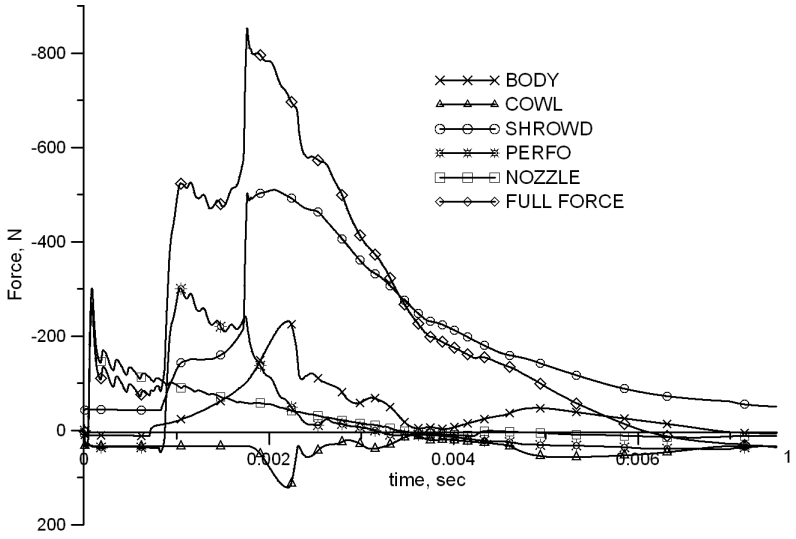

Figure 8: Balance of longitudinal forces for variant 2, α=1, β=0.2, θ=135º.

In spite of high useful force, in the variant 2 the compression wave still came out from the inlet – see Fig. 5. While the compression wave is moving along the perforated section, it becomes weaker. But the bypass of the gas inside the shroud results in formation of the secondary shock wave, which moves in the same direction as the shock wave in the main duct. This secondary wave even slightly outruns the main wave (it is moving along the shroud, where the gas is practically at rest, while the wave in the main duct is moving against the current). It turned out that the reflection of the compression wave from the bypass shroud end-wall leads to a strong growth of its intensity. As a result, the inverse flow of gas from the shroud to the main duct arises, and a new shock wave is formed in the main duct. This new wave is sufficiently strong to pass further upstream towards the inlet. In order to diminish this effect, the third variant of geometry was considered, in which the bypass shroud was divided into three rings – 3b, 3c and 3d (Fig.4). The shroud was divided to get several sequential reflections of the compression wave from the bypass shroud end-walls and thus to diminish the compression wave intensity after its reflection from the shroud end-wall in the last ring (ring 3b). For the final damping of the compression wave, one more section (3a) has been added; it contained perforation in the outer wall of the shroud.

Calculations were performed with the same fuel consumption as in calculations of the variant 2. As a result, the useful force $\langle R \rangle$ has diminished 1.5 times in comparison with the variant 2, while the outer drag increased. But the compression wave has stopped just after its entrance in the section 3a. In this case the specific impulse $J_{sp} = 12794$ sec and the useful force coefficient $C_R = 0.76$ were obtained – see the Table 1. These characteristics are worse than in the variant 2, but the compression wave is prevented from coming to inlet – see Fig.5.

The analysis of different components of longitudinal force demonstrates that in variant 1 the perforated wall mainly produces drag (fig.9). On the contrary, in variant 2 it gives considerable input into the thrust, comparable with the input of the force which appears when the secondary shock wave

reflects from the bypass shroud end-wall. After this reflection useful force generated by the perforated wall comes to naught quickly, whereas the bypass shroud end-wall still produces thrust for a long time. In variant 3 the principal input into the thrust is generated by the walls of bypass shrouds; at the same time, small useful input is generated by the perforated wall.

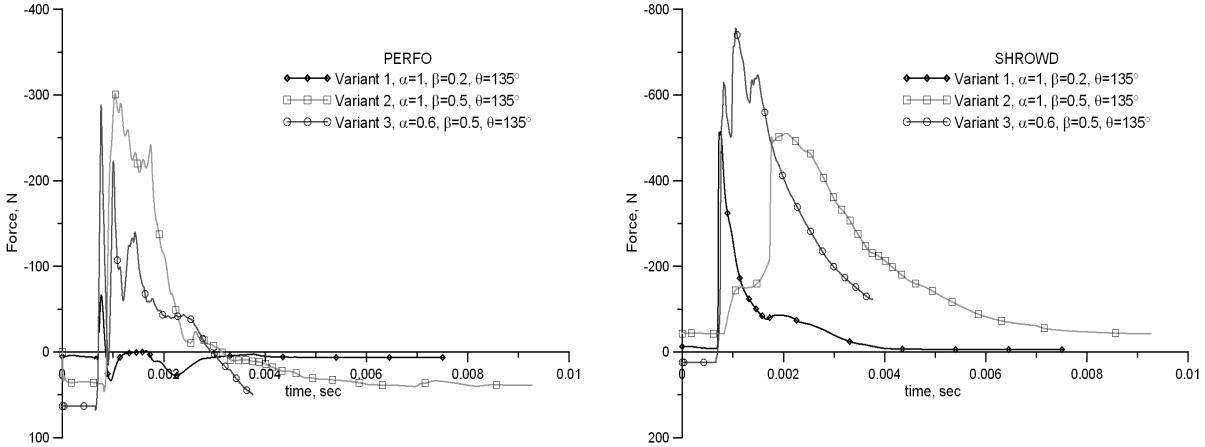

Figure 9: Time dependence of longitudinal force (H), acting on some elements of construction.

It is also worth mentioning that in the variant 3 the flow inside the chamber appears to be supersonic at the end of cycle. It leads to worse mixing of fuel with air and, possibly, to worse characteristics of the following working cycles of the engine. This problem should be solved in the future.

4 Concluding remarks

Presented results show that the considered concept of ramjet-type PDE has enough resources to obtain the useful force that would be several times higher than the outer drag. Necessity to damp the shock wave leads to diminishing the PDE useful characteristics, but the damping losses may be optimized. In all considered variants of the PDE geometry, the working frequency of the device was higher than 100 Hz.

The obtained results are not final ones. Additional investigations are necessary for optimization of the damping process, for taking into account the viscous effects. In the variant 3, additional efforts are necessary to keep the subsonic character of flow inside the combustor during the duct filling by fuel.

References

[1] Remeev N.Kh., Vlasenko V.V., Khakimov R.A. Analysis of operation process and possible performance of the supersonic ramjet-type pulse detonation engine. Pulse and Continuous Detonation Propulsion, Ed. By G.Roy, S. Frolov, J. Shepherd, Moscow, Torus Press, 2005, pp.257-272.

[2] Confined Detonation and Pulse Detonation Engines. Ed. by G.Roy, S.Frolov, R.Santoro, S.Tsyganov. Torus Press, Moscow, 2003.

[3] K.Kailasanath. Recent Developments in the Research on Pulse Detonation Engines. AIAA Journal, vol.41, No2, February, 2003.

[4] Y.Wu, F.Ma and V.Yang. Sustem Performance and Thermodynamic Cycle Analysis of Air breathing Pulse Detonation Engines. J. of Propulsion and Power, vol.19, No.4, July-August, 2003.

[5] Remeev N.Kh., Vlasenko V.V., Khakimov R.A., Ivanov V.V. Numerical Simulation and Experimental Investigation of Operation Process in a Detonation Combustor. Intern. Colloq. on Advances in confined Detonation. Ed. by G.Roy, S.Frolov, R.Santoro, S.Tsyganov. Book of Abstracts. Torus Press, Moscow, 2003, pp.238-242.

[6] Remeev N.Kh., Vlasenko V.V., Khakimov R.A. Numerical Simulation and Experimental Investigation of Working Process in a Model of Ramjet–Scheme Pulsing Detonation Engine. In the book: “Pulsing Detonation Engines”. Ed. by S.M.Frolov, Moscow, Torus Press, 2006, pp. 311-348. (In Russian.)